LUPINE PUBLISHERS

Interventions in Gynaecology & Women's Healthcare

DOI: 10.32474/IGWHC.2022.05.000206

ISSN: 2637-4544

Research Article

# Circ_0001529 Expression Abnormalities Mediate the miR-578 CDC25A Axis Involved in the Growth of Ovarian Cancer

**Yang Rao[1], Wenwen Zhang[2], Dan Li[3], Xiao Li[1], Yaomei Ma[3]* and Pengpeng Qu[1]***

[1]*Department of Gynecological Oncology, Tianjin Central Hospital of Gynecology and Obstetrics, China*

[2]*Research Institute of Obstetrics and Gynecology, Tianjin Central Hospital of Gynecology and Obstetrics, China*

[3]*Department of Gynecological Oncology, Tianjin Medical University Cancer Institute & Hospital, China*

***Corresponding author:** Yaomei Ma, Department of Gynecological Oncology, Tianjin Medical University Cancer Institute & Hospital, No.45 Binshui Road, Hexi District, China and Pengpeng Qu, Department of Gynecological Oncology, Tianjin Central Hospital of Gynecology and Obstetrics, Huanhu West Road, China

**Received:** January 14, 2022 **Published:** January 25, 2022

## Abstract

**Purpose:** To investigate the effect of Circ_0001529-mediated miR-578-CDC25A axis on the growth of ovarian cancer cells in vitro and in vivo.

**Method:** The expression differences of Circ_0001529 in ovarian cancer tissues and paraneoplastic tissues were first analyzed; Circ_0001529 overexpression plasmids and interference plasmids were constructed and transfected into SKOV3 cells and SiHa cells, respectively, followed by MTT assay, flow cytometry, and immunofluorescence to detect cell growth, proliferation, and apoptosis. The binding relationship between Circ_0001529 and miR-578, or miR-578 and CDC25A was verified by online prediction site and dual luciferase assay, and CDC25A overexpression plasmid and interference plasmid were constructed and transfected into SKOV3 cells and SiHa cells, respectively. qRT-PCR and Western Blot were used to to detect the expression of ACP5, followed by cell growth as well as apoptosis. A mouse xenograft tumor model was constructed, and the growth of ovarian cancer cells in vivo was assessed by calculating tumor volume growth with KI67 and Caspase-3 immunohistochemistry.

**Result:** Circ_0001529 was highly expressed in ovarian cancer tissues and cells; silencing Circ_0001529 inhibited ovarian cancer cell growth and promoted apoptosis in vitro and in vivo. circ_0001529 could bind to miR-578 target, and miR-578 bound to CDC25A mRNA target. Overexpression of Circ_0001529 promotes the expression of CDC25A and promotes the growth and inhibits the apoptosis of ovarian cancer cells. CDC25A can upregulate the ERK/MAPK signaling pathway, thus promoting ovarian carcinogenesis.

**Conclusion:** circRNA_0001529 promotes CDC25A expression through targeted binding of miR-578, thereby promoting the growth and metastasis of ovarian cancer cells.

**Key words:** ACP5; Circ_0001529; Lung Carcinoma; Kalpan-Meier Analysis; Proliferation; Apoptosis; Erk/Mapk Signaling Pathway

## Introduction

Ovarian cancer (OC) is one of the deadliest gynecological cancers, with a significant fatality rate. It has a poor prognosis due to late diagnosis and medication resistance [1]. In the treatment of ovarian cancer, it is critical to distinguish between patients who will benefit from primary full cytoreductive surgery and those who will benefit more from neoadjuvant chemotherapy [2]. TK1 could be used as a biomarker to diagnose ovarian cancer. When it comes to differentiating malignant ovarian tumors from benign ones, ROMI outperforms ROMA [3]. The use of cytoreductive surgery (CRS) with hyperthermic intraperitoneal chemotherapy (HIPEC) has been demonstrated to be effective in a variety of cancers, and it may also provide a prognosis benefit for patients with advanced ovarian cancer [4]. The intracellular signal transducer and regulator of gene expression and protein turnover, Focal adhesion Kinase (FAK), increases tumor progression and is a promising therapeutic target for a variety of cancers, including ovarian cancer. [5] There have

been some results suggesting that ERRα may promote ovarian cancer progression and may serve as a promising predictive biomarker [6]. Ovarian Cancer (OC) is a type of gynecological cancer with high mortality rate, and Circ_000152. (PM9 plays an important role in it. However, the clinical significance of circular RNA and its molecular mechanism in OC are mostly unknown. Circ_0001529 (hsa_circAFF4_016), is a circular RNA formed by reverse shearing of AFF4, is a circular RNA newly discovered by us [7] Circular RNAs (circRNAs) are increasingly recognized as important regulators in cancer including ovarian cancer (OC). This work focuses on the effects of circ_0000745 on the OC development of and molecules involved [8]. Imaging intracellular microRNAs (miRNAs) demonstrated an essential role in exposing their biological and pathological functions [9]. The induction of microribonucleic acid (miRNA) in cells is of great significance for early disease diagnosis and treatment monitoring. DNA is an interesting building material that can be programmed into components with rigid and branched structures and is particularly suitable for intracellular biomolecular imaging or therapeutic drug delivery [10]. Moreover, it has been shown that targeting the hsa_circ_0005785/miR-578/APRIL regulatory pathway may be a promising diagnostic and therapeutic strategy in the clinical practice of HCC [11]. Similarly, for the ovarian cancer we studied, we combined Circ_0001529 with miR-578 targeting to see if it could promote cancer cell changes and metastasis functionally. Given the importance of silencing Circ_0001529 in ovarian cancer treatment, we aimed to identify an excellent inhibitor and investigate its potential therapeutic effects, thereby knocking down the role of Circ_0001529 expression to promote ovarian cancer cell growth and inhibit its apoptosis. Circular RNA (circRNA) is recently found to participate in the regulation of tumor progression, including ovarian cancer.

## Methods

### Tissue samples

Eighty patients with ovarian cancer diagnosed and treated in our hospital from September 2012 to June 2013 were selected from surgically resected cancerous tissue and normal paracancerous tissue (at least 2 cm away from the ovarian cancerous tissue), with a median age of 49-79 years and a mean age of (64.9± 7.3) years. And all patients were followed up every three months for five years. Inclusion criteria: 1, all patients were diagnosed with ovarian cancer by postoperative pathological examination; 2, all patients did not receive radiotherapy or chemotherapy before surgery; 3, clinical data were complete. Exclusion criteria: 1, combined with chronic systemic diseases; 2, combined with other malignant tumors. The study was approved by our ethics committee and supervised by our ethics committee, and the subjects all signed the informed consent form while enjoying the right to information.

### Cell Culture

Human ovarian cancer cell lines Hela, SKOV3, SiHa, SPC-A-1, L9981 and human normal ovarian epithelial cells HOSE-1 were purchased from the Tumor Cell Bank of China Medical College (Beijing, China), and subsequently inoculated into cell culture dishes at a density of $1\times10^5$ cells/cm2 using RPMI-1640 medium containing 10% fetal bovine serum, CM7-1 medium, F12K medium and LHC-9 medium (all purchased from Gibco, Grand Island, NY,USA), and cultured at 37°C , 5% CO2 for 48 h until cell growth was fused to 80%-90%, digested with 0.025% trypsin (Gibco), and passaged.

### qRT-PCR

Total RNA of tumor tissues and cells was used using RNAiso Plus (TAKARA, Otsu, Shiga, Japan) and Trizol LS Reagent (TAKARA, Otsu, Shiga, Japan), respectively. The reliability of the obtained RNA was subsequently verified using formaldehyde denaturation electrophoresis assay to continue the subsequent experiments. Reverse transcription polymerase chain reaction (RT-PCR) experiments were then performed using the PrimeScript ™RT kit (TAKARA, Otsu, Shiga, Japan) strictly according to the instructions. The mRNA expression levels were quantified by standard real-time quantitative PCR methods using SYBR Premix Ex Taq (TAKARA, Otsu, Shiga, Japan). gAPDH was used as a reference gene. The primers for each group are shown in Table 1.

**Table 1:** qRT-PCR primer sequences.

| Primer | Sequence |
|---|---|
| CDC25A-F | AGATCCTGGGTGCAGACTTC |
| CDC25A-R | GTAGAAAGGGCTGGGGAAG |
| Circ_0001529-F | CAGGCAGATCCAGCCATC |
| Circ_0001529 -R | TTGAGAGTCGACTGGAAAGTTCT |
| GADPH-F | ACAGTCAGCCGCATCTTCTT |
| GADPH-R | GACAAGCTTCCCGTTCTCAG |

### Immunoblot

**Table 2:** Antibodies used in western blot experiments.

| Name of antibody | Article number and Company | Dilution ratio |
|---|---|---|
| β-actin | ab179467, abcam | 3.513888889 |
| CDC25A | Ab191406, ABcam | 0.736111111 |
| MAPK | Ab185145, ABcam | 0.736111111 |
| p-MAPK | Ab59479, ABcam | 0.736111111 |
| ERK | Ab53277, ABcam | 0.736111111 |
| p-ERK | Ab74032, ABcam | 0.736111111 |
| PUMA | Ab9643, ABcam | 01:50 |
| Bax | Ab32503, ABcam | 3.513888889 |
| P53 | Ab32389, ABcam | 0.736111111 |

Total proteins were extracted by RIPA lysis buffer containing PMSF (Beyotime, Beijing, China). The supernatant protein levels were determined by standard BCA assay. Equal amounts of protein (50 mg) were loaded onto 10% sodium dodecyl sulfate polyacrylamide gel electrophoresis (SDS-PAGE) and then transferred onto PVDF membranes (Millipore, Billerica, MA, USA) after electrophoresis. The PVDF membranes were incubated with

TBST (Boster, Wuhan, China) using also 5% skimmed milk at room temperature to block non-specific binding. The membranes were then incubated with primary antibodies (Table 2) separately at 4°C overnight. The rabbit anti-mouse secondary antibody was then incubated for 1 h at room temperature. The membranes were visualized by electrochemiluminescence (ECL) and imaged using a BioSpectrum gel imaging system (Bio-Rad, Hercules, CA, USA).

### MTT

Cells in good growth condition were taken from each group, and cell activity was detected using MTT Cell Proliferation and Cytotoxicity Assay Kit (C0009, Biyuntian, Shanghai). All operations were performed strictly according to the instructions.

### Flow Cytometry

**Cell proliferation:** Cells of each group in good growth condition were taken, washed with PBS, digested with 0.025% trypsin, and incubated with DMEM containing 2 mmol of CFSE (Invitrogen) for 15~30 min. Cells were washed with PBS three times, centrifuged, supernatant was discarded, DMEM was added to resuspend the cells, and detected on the machine.

**Cell cycle:** cell suspensions were taken, and cells were treated with 70% methanol (v/v) at -20°C for 24 h. Subsequently, PI (50μg/mL) containing 10μg/mL of RNase was added to treat the cells for 20 min. finally, the distribution of cell cycle was detected on the machine.

**Apoptosis:** 5μL each of Annexin V-FITC and PI were added to the cell suspension and incubated in the dark for 10 min. after staining was completed, apoptosis was detected on the machine.

### Immunofluorescence

Groups of cells grown on glass coverslips were rinsed, washed three times with PBS, and fixed with 4% paraformaldehyde at 4°C for 15 min. The cells were treated with 0.5% Triton-100 X for 20 min. PCNA primary antibody (1:200, ab92552, ABcam), Cytochrome C primary antibody (1:100, ab133504, ABcam) were added separately and incubated overnight at 4°C. The cell crawls were washed with PBS, and Alexa Fluora 594-labeled sheep anti rabbit secondary antibody (1:5000, ab150088, ABcam) was incubated at 37°C for 1h. Cells were subsequently visualized using a DAPI re-stained cell nuclear fluorescence microscope (Leica DM 3000). Mitochondrial staining was performed using Mito Tracker TMRed CMXRos-Special Pcakaging (M7512, ThermoFisher, CA), and all operations were performed strictly according to the instructions.

### PI staining

Cells in good growth condition were taken from each group, and the cells were fixed with 4% paraformaldehyde for 20 min, and then stained with PI (propidium iodide) (3μM) for 5 min in the dark. Finally, the cells were analyzed by fluorescence microscopy. Five areas in each group were randomly selected for analysis. Apoptotic cell nuclei were stained red.

### Establishment Of a Mouse Allograft Tumor Model

Thirty SPF-grade nude mice (4-6 weeks old, 20+2 g, strain: BALB/c Nude) (purchased from Beijing Viton Lihua Laboratory Animal Technology Co., Ltd, Beijing, China, Animal License No.: SCXK (Beijing) 2015-0001) were numbered by body weight as a parameter and divided into 6 groups of 5 animals each at random numbers. $4 \times 10^6$ Blank, NC and si-ACP5 groups of transfected stable SiHa cells and Blank, NC and OE-ACP5 groups of transfected stable SKOV3 were dispersed with 2mL saline and injected subcutaneously into each group of nude mice one by one correspondingly. Seven days after injection, the tumor volumes of mice were measured every 7 days (the volume of tumors was calculated by the formula: $m_1^2 \times m_2 \times 0.5236$[12], with $m_1$ representing the shortest axis and $m_2$ representing the longest axis), and the mice were executed after 28 days, and the tumors were removed for weighing and then subjected to histological experiments. The allograft tumor tissues from each group of mice were extracted and the tissues were sectioned using frozen sections. Five randomly and equally spaced sections were selected for immunohistochemical experiments.

### Immunohistochemistry

Tissue sections were routinely processed [13] and incubated with KI67 primary antibody (1:500, ab15580, ABcam) and Caspase-3 (1:1000, ab13847, ABcam) primary antibody for 30 min, washed 3 times with PBS, and incubated dropwise with 40μL of horseradish enzyme-labeled streptavidin working solution at 37°C for 15 min. The sections were washed three times with PBS, subjected to DAB color development reaction, rinsed with distilled water and then restrained with hematoxylin for 30s. The sections were sealed with neutral gum after dehydration. Five non-overlapping fields were selected for observation under the microscope in each section. Cells showing brownish-yellow or brownish-brown granules in the nucleus were positive for KI67 or Caspase-3. In each section, five areas were randomly selected respectively, and the proportion of positive cell numbers was counted.

### Data analysis

SPSS 21.0 (SPSS, Inc, Chicago, IL, USA) statistical software was used to analyze the data. Data were normally distributed by Kolmogorov-SmiRnov test, and results were expressed as mean ± standard deviation. t-test was used for comparison between two groups, One-Way ANOVA one-way ANOVA was used for comparison between multiple groups, and Tukey's multiple comparisons test. survival curves were tallied by Kalpan-Meier method, and log rank test was used for post-statistical analysis. p was a two-sided test, and differences were considered statistically significant at $p < 0.05$.

## Results

### Circ_0001529 was highly expressed in ovarian cancer tissues and cells

Circ_0001529 was significantly highly expressed in ovarian cancer tissues (Figure1A) by online database analysis, while in a

previous study it was shown that Circ_00015295 was significantly highly expressed in liver cancer patients and promoted the growth of liver cancer cells [14]; the expression level of Circ_0001529 in cancer tissues of 80 ovarian cancer patients was significantly higher than that of paraneoplastic tissues (Figure 1B); the analysis of the relationship between the expression of Circ_0001529 and the clinical characteristics of ovarian cancer patients showed that (taking Circ_0001529 as the In 80 ovarian cancer patients, the expression level of Circ_0001529 was significantly higher than that of paraneoplastic tissues (Figure 1B); analysis of the relationship between the expression of Circ_0001529 and clinical characteristics of ovarian cancer patients showed that (the median relative expression of Circ_0001529: 5.53, patients with relative expression of Circ_0001529 below 5.53 were considered as low In ovarian cancer tissues, the expression of Circ_0001529 was related to the clinical stage, lymph node metastasis and tumor differentiation of patients; the expression level of Circ_0001529 increased with the clinical stage of ovarian cancer, and the expression level of Circ_0001529 in cancer tissues of stage III+IV patients was significantly higher than that of stage I+II patients. The expression level of Circ_0001529 was significantly higher in stage III+IV patients than in stage I+II patients ($P < 0.05$); the expression level of Circ_0001529 was significantly higher in cancer tissues of patients with low differentiation than in patients with high differentiation ($P < 0.05$); the expression level of ACP5 was significantly higher in cancer tissues with lymph node metastasis than in cancer tissues without lymph node metastasis ($P < 0.05$).Circ _0001529 expression was not significantly related to either age or tumor size (all $P > 0.05$) (Table 3). Subsequently, we performed Kalpan-Meier survival analysis of patients based on follow-up records, which showed that patients with high Circ_0001529 expression had a worse prognosis with a five-year survival rate of 15.0% and a mean survival time after diagnosis of 27.1 months, whereas in patients with low ACP5 expression had a relatively good prognosis with a five-year survival rate of 30.0% and a mean survival time after diagnosis of survival of 40.4 months (all $P < 0.05$) (Figure 1C).

To further verify the role of Circ_0001529 in ovarian cancer, qRT-PCR results showed that the expression of ACP5 was significantly higher in ovarian cancer cells Hela, SKOV3, SPC-A-1, and SiHa than in HOSE-1 cells (Figure 1D). By constructing Circ_0001529 overexpression vector, transfected into SKOV3 cells with low relative expression of Circ_0001529; constructing Circ_0001529 small interfering RNA (small interfere RNA) transfected into SiHa cells with the highest relative expression of Circ_0001529. qRT- PCR results showed that the expression of Circ_0001529 was interfered with, indicating successful transfection (Figure 1E & 1F).

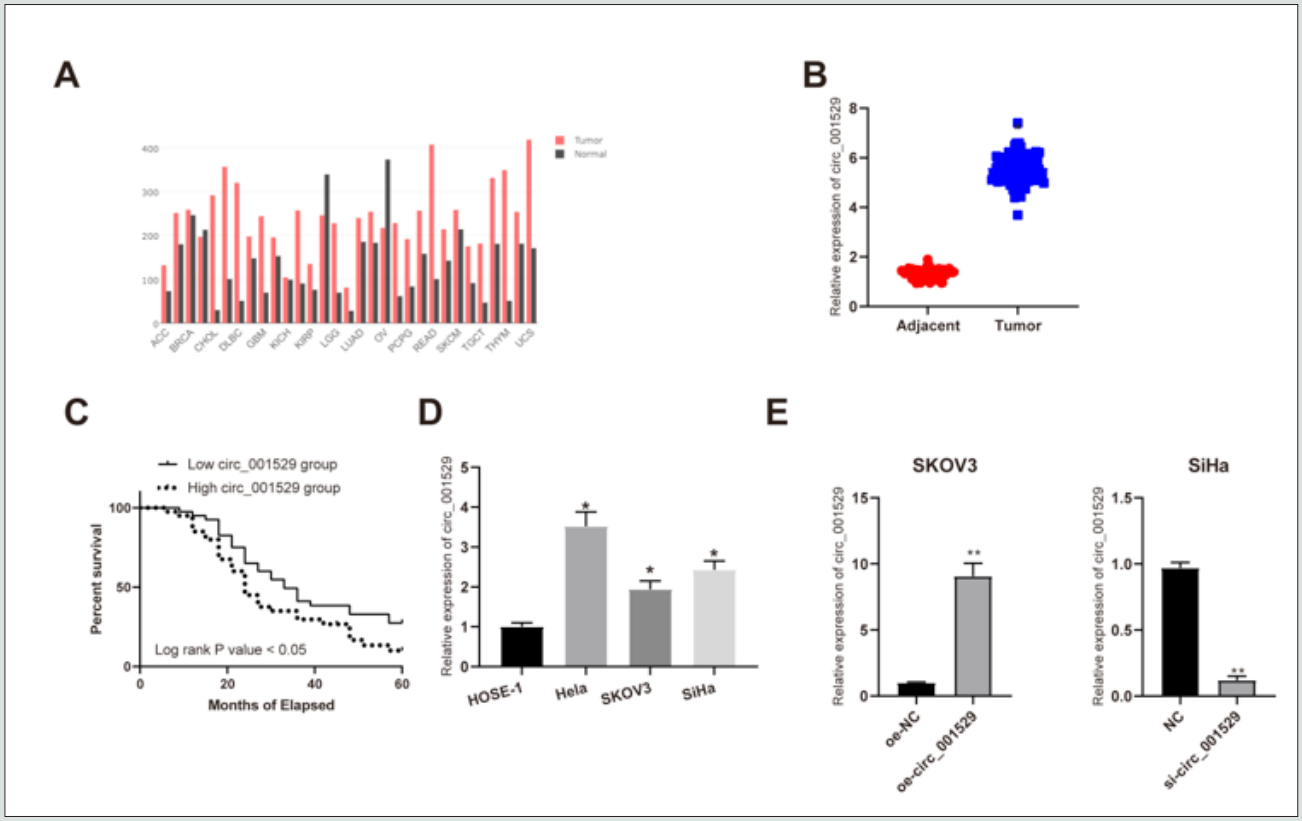


**Figures 1:** The expression level of Circ_0001529 was significantly higher in ovarian cancer tissues. (A) Circ_0001529 was significantly highly expressed in both ovarian cancer tissues; (B) Ovarian cancer cells; (C) Kalpan-Meier survival analysis; (D) Expression levels of Circ_0001529 in SKOV3 cells; (E) SiHa cells after transfection.

**Table 3:** Relationship between the expression level of ACP5 in tumor tissues and clinical characteristics of ovarian cancer patients {n (%)}.

| Clinical Information | Number Of Cases | Expression levels of Circ_0001529 in tumor tissues | | P value |
|---|---|---|---|---|
| | | Low expression (n=40) | High expression (n=40) | |
| **age** | | | | |
| ≤ 65 years | 38 | 18 (45.5) | 20 (50.0) | 0.823 |
| > 65 years old | 42 | 22 (54.5) | 20 (40.0) | |
| **Tumor diameter** | | | | |
| ≤ 5 cm | 33 | 17 (42.5) | 16 (40.0) | 0.999 |
| > 5 cm | 47 | 23 (57.5) | 24 (60.0) | |
| **clinical staging** | | | | |
| I + II | 24 | 18 (75.0) | 6 (25.0) | 0.012 |
| III + IV | 56 | 21 (37.5) | 35 (63.5) | |
| **lymph node metastasis** | | | | |
| not | 48 | 13 (32.50) | 32 (87.5) | < 0.001 |
| have | 32 | 27 (67.50) | 8 (12.5) | |
| **Degree of differentiation** | | | | |
| low level | 8 | 1 (12.5) | 7 (87.5) | < 0.001 |
| high level | 72 | 39 (51.42) | 33 (48.58) | |

## Overexpression of ACP5 promotes the growth and inhibits the apoptosis of ovarian cancer cells

The results of MTT assay for cell activity showed that: in SKOV3 cells, overexpression of Circ_0001529 significantly elevated cell activity; while inhibition of Circ_0001529 expression in SiHa cells significantly decreased cell activity (Figure 2A). Flow cytometry assay of cell proliferation showed that: overexpression of Circ_0001529 in SKOV3 cells significantly elevated cell proliferation, while inhibition of Circ_0001529 expression in SiHa cells significantly decreased cell proliferation (Figure 2B). Proliferation cell nuclear antigen (PCNA) is only present in cells undergoing mitosis and the level of phase expression represents the level of cell proliferation capacity [15] PCNA staining showed that in SKOV3 cells, overexpression of Circ_ 0001529, the number of positive cells was significantly increased, while inhibition of Circ_0001529 expression in SiHa cells resulted in a significant decrease in the number of positive cells (Figure 2C).

Flow cytometry detection of apoptosis in each group showed that in SKOV3 cells, overexpression of Circ_0001529 significantly decreased the number of apoptotic cells, while inhibition of Circ_0001529 expression in SiHa cells significantly increased the number of apoptotic cells (Figure 2D). PI staining results showed that in SKOV3 cells, overexpression of Circ_ 0001529, the number of nuclei of sequestered cells was reduced, while inhibition of Circ_0001529 expression in SiHa cells increased the number of damaged nuclei (Figure 2E). The western blot assay of apoptosis-related proteins Bax1, PUMA, and Cleaved caspase-3 showed that overexpression of Circ_0001529 in SKOV3 cells significantly decreased the expression level of apoptosis-related proteins, while inhibition of Circ_0001529 expression in SiHa cells significantly increased the cellular expression level of apoptosis-related protein expression level was significantly elevated by inhibition of Circ_0001529 expression in SiHa cells (Figure 2F). Flow cytometry detection of cell cycle distribution showed that in SKOV3 cells, overexpressing Circ_0001529, the cells did not have cycle arrest; while inhibiting the expression of Circ_0001529 in SiHa cells, the G2/M phase cells were significantly increased, indicating that inhibiting the expression of Circ_0001529 promoted G2/M phase cycle arrest (Figure 2G).

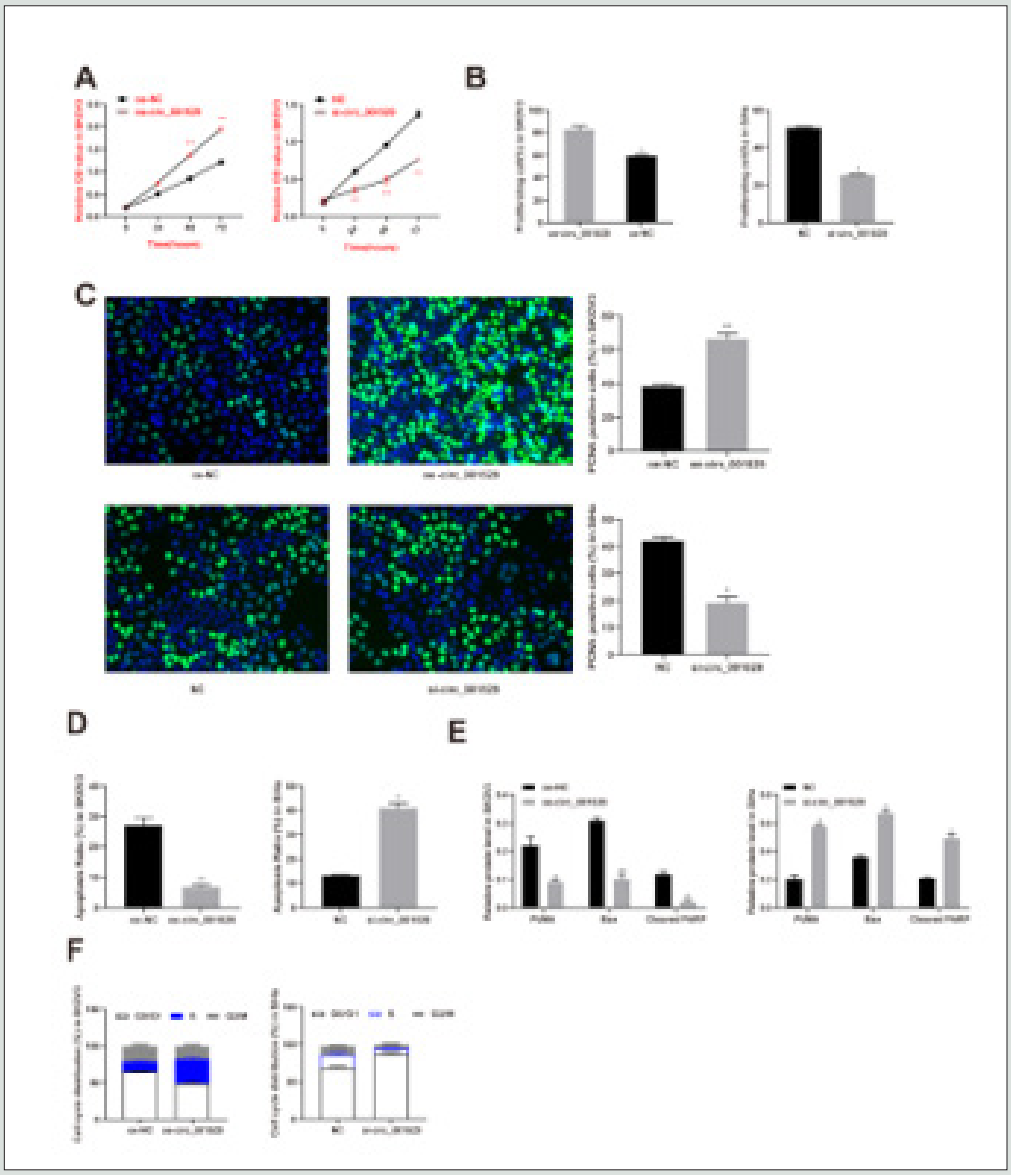


**Figures 2:** (A) MTT assay for cell activity; (B) Cell proliferation; (C) PCNA immunofluorescence staining; (D) Apoptosis; (E) PI staining; (F) Apoptosis-associated protein assay; (G) Cell cycle distribution.

## Circ_0001529 promotes CDC25A expression by targeting binding to miR-578

We found miR-578 could act on Circ_00015293'-UTR sequence (Figure 3A) through online prediction website, and the action site is shown in Figure 3B. Subsequent correlation analysis of miR-578 expression levels with those of Circ_0001529 in tumor tissues of clinically collected ovarian cancer patients showed a negative correlation (Figure 3C). And the results of double luciferase assay showed that Circ_0001529 could indeed bind to miR-578 target (Figure 3D). And qRT-PCR detected the expression of miR-578, and the results showed that silencing the expression of Circ_0001529 led to an increase in the expression level of miR-578 (Figures 3E & 3F). We further analyzed and found that miR-578 could target binding to the 3'-UTR sequence of CDC25A mRNA (Figure 3G), so we further found that mIR-578 could target binding to CDC25A by dual luciferase assay. We also found that the expression level of miR-578 was negatively correlated with that of CDC25A and positively correlated with that of Circ_0001529 in clinical samples (Figure 3H).

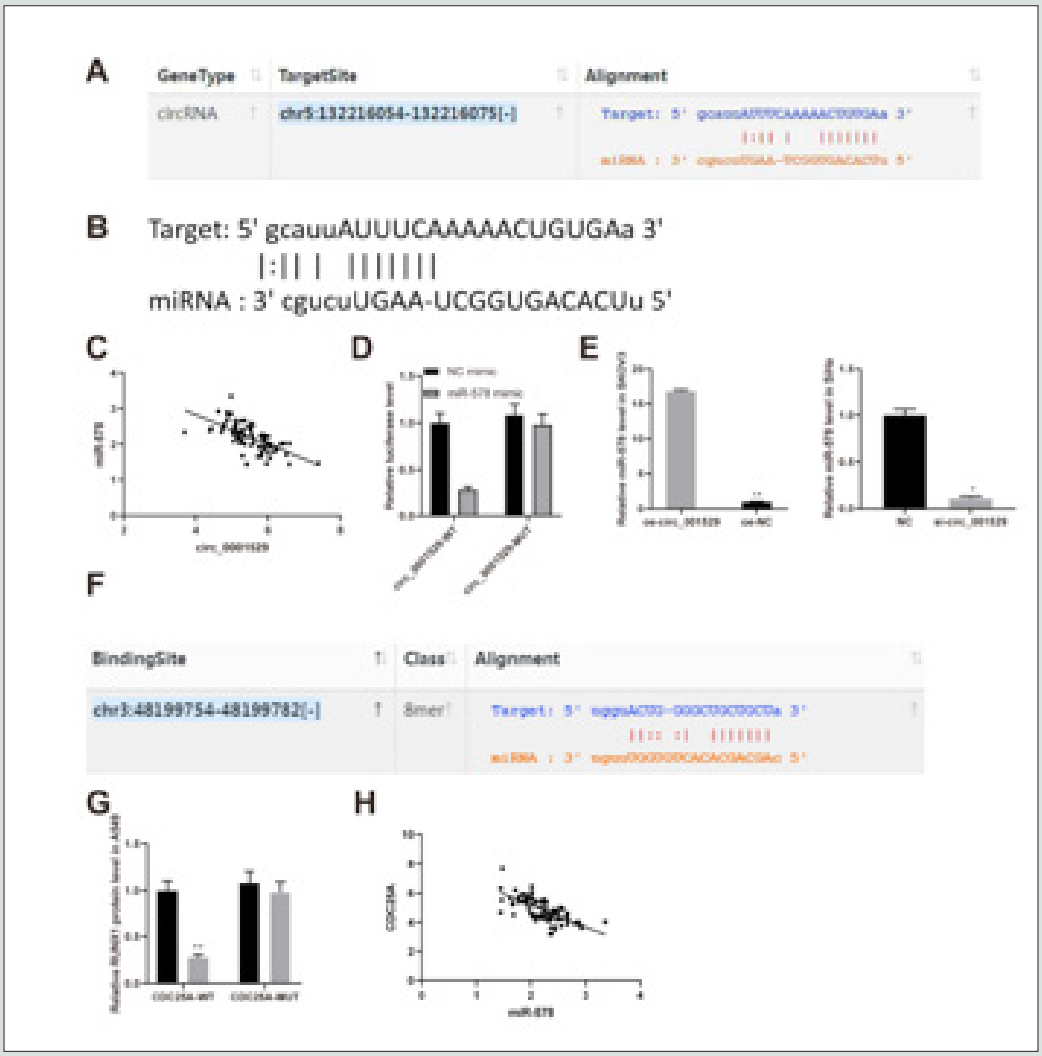


**Figures 3:** Circ_0001529 promotes CDC25A expression by targeting binding to miR-578. (A~B), Starbase and circbank websites predicted the binding site of Circ_0001529 to miR-578; (C) Correlation analysis of miR-578 expression level with that of Circ_0001529 in tumor tissues of clinically collected ovarian cancer patients; (D) Dual luciferase assay to analyze the binding relationship between Circ_0001529 and miR-578 binding relationship; (E) qRT-PCR to detect the expression level of miR-578; (F~G) Double luciferase assay to analyze the binding relationship between CDC25A and miR-578, (H) Correlation analysis of the expression level of miR-578 with that of CDC25A in tumor tissues of clinically collected ovarian cancer patients.

## Silencing CDC25A inhibits proliferation and promotes apoptosis in ovarian cancer cells

The results of MTT assay for cell activity showed that overexpression of CDC25A in SKOV3 cells significantly elevated cell activity, while inhibition of CDC25A expression in SiHa cells significantly decreased cell activity (Figure 4A). Flow cytometry results for cell proliferation showed that overexpression of CDC25A in SKOV3 cells significantly elevated cell proliferation, while inhibition of CDC25A expression in SiHa cells significantly decreased cell proliferation (Figure 4B). PCNA staining results showed that overexpression of CDC25A in SKOV3 cells significantly increased the number of positive cells, while inhibition of CDC25A expression in SiHa cells resulted in a significant decrease in the number of positive cells (Figure 4C).

Flow cytometry detection of apoptosis in each group showed that overexpression of CDC25A in SKOV3 cells significantly decreased the number of apoptotic cells, while inhibition of CDC25A expression in SiHa cells significantly increased the number of apoptotic cells (Figure 4D). PI staining showed that overexpression of CDC25A in SKOV3 cells decreased the number of nuclei of sequestered cells, while in SiHa cells the expression of CDC25A was inhibited and the number of damaged nuclei was increased (Figure 4E). The western blot detection of apoptosis-related proteins Bax, PUMA, and Cleaved caspase-3 showed that

overexpression of CDC25A in SKOV3 cells significantly decreased the expression level of apoptosis-related proteins, while inhibition of CDC25A expression in SiHa cells significantly increased the expression level of apoptosis-related proteins in the cells (Figure 4F). Flow cytometry detection of cell cycle distribution showed that in SKOV3 cells, overexpressing Circ_0001529, the cells did not have cycle arrest, while inhibition of CDC25A expression in SiHa cells significantly increased G2/M phase cells, indicating that inhibition of CDC25A expression promotes G2/M phase cycle arrest (Figure 4G).

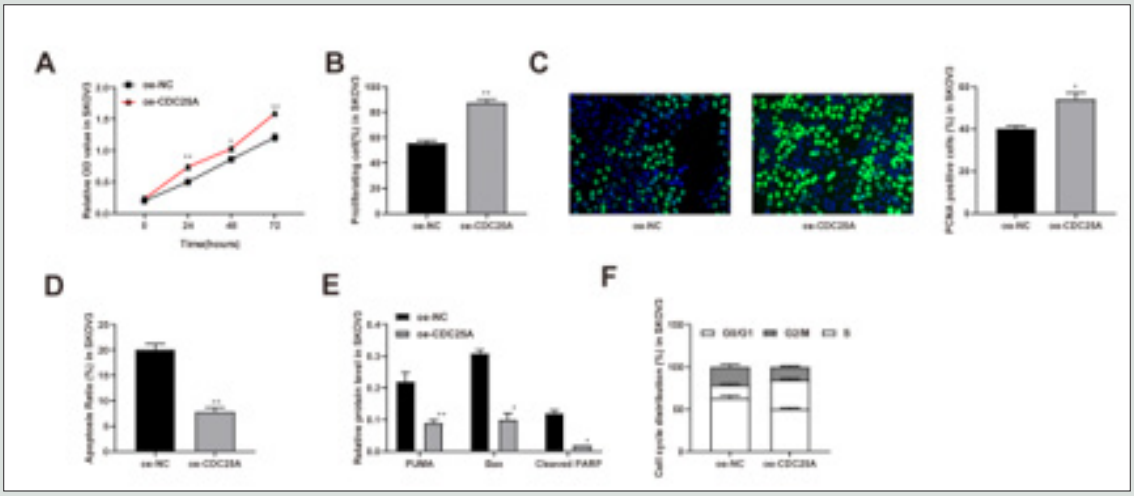


**Figures 4:** (A) MTT assay for cell activity; (B) Cell proliferation; (C) PCNA immunofluorescence staining; (D) Apoptosis; (E) PI staining; (F) Apoptosis-associated protein assay; (G) Cell cycle distribution.

## Overexpression of CDC25A partially alleviates the suppression of ovarian cancer cell activity caused by silencing Circ_0001529

To further verify the role of ACP5 in ovarian cancer, we constructed a CDC25A overexpression vector and cotransfected it into si-Circ_0001529 SiHa cells. qPCR and western blot results showed that the transfection was successful (Figures 5A & 5B). After overexpression of CDC25A, cell activity and proliferation rate were significantly enhanced (Figures 5C-5E); apoptosis was significantly attenuated (Figures 5F-5H); cell cycle arrest was effectively alleviated (Figure 5I).

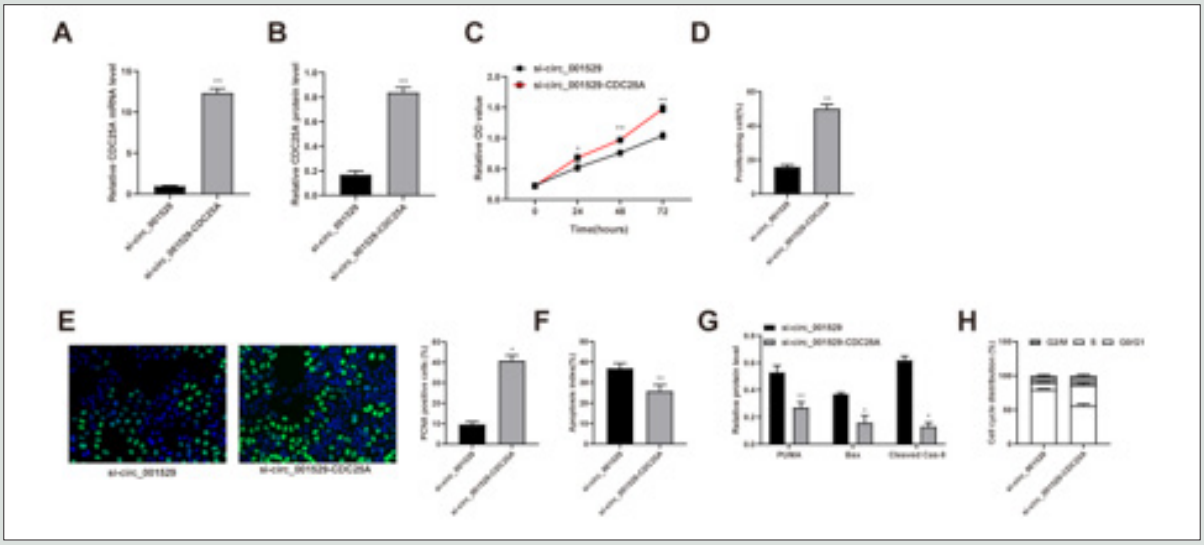


**Figures 5:** (Overexpression of CDC25A partially alleviates the suppression of ovarian cancer cell activity caused by silencing Circ_0001529. (A) CDC25A mRNA levels; (B) Protein levels in cells; (C) MTT assay for cell activity; (D) Cell proliferation; (E) PCNA immunofluorescence staining; (F) apoptosis; (G) CytC staining; (H) Apoptosis-associated protein assay; (I) Cell cycle distribution.

### Overexpression of Circ_0001529 promotes the growth of heterotrophic tumors in mice in vivo

The results of measuring the growth of xenograft tumors in mice showed that the volume growth and weight of xenograft tumors were significantly elevated by overexpression of Circ_0001529 in SKOV3 cells, while the volume growth and weight of xenograft tumors were significantly inhibited by inhibition of Circ_0001529 expression in SiHa cells (Figures 6A&6B); immunohistochemical detection of The expression of KI67 and Caspase-3 in heterotopic tumor tissues showed that overexpression of Circ_0001529 in SKOV3 cells significantly elevated the KI67 positivity rate and significantly decreased the Caspase-3 positivity rate in heterotopic tumors; inhibition of Circ_0001529 expression in SiHa cells, the heterotopic tumor KI67 positivity was significantly reduced, while Caspase-3 positivity was significantly elevated (Figure 6C).

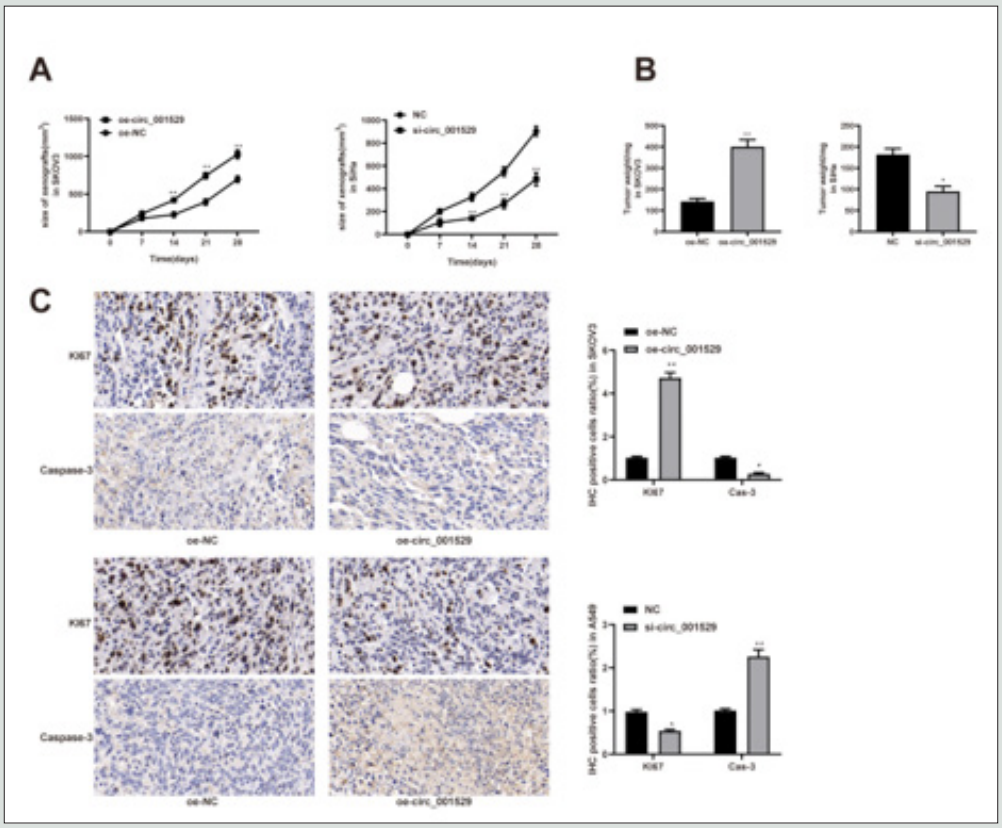


**Figures 6:** Overexpression of Circ_0001529 promotes heterotopic tumor growth in mice in vivo. (A) Heterotrophic tumor volume growth curve; (B) Tumor weight; KI67 and (C) Caspase-3 immunohistochemistry.

### CDC25A promotes ovarian carcinogenesis through upregulation of ERK/MAPK signaling pathway

ERK/MAPK was significantly highly expressed in most cancers, so we used Western Blot to detect the expression level and phosphorylation level of ERK/MAPK in cancer tissues and paracancerous tissues, and the results showed that ERK/MAPK phosphorylation level was significantly higher in cancer tissues than in paracancerous tissues (Figure 7A). And, in SKOV3 cells, overexpression of circ_0001529 significantly increased ERK/MAPK phosphorylation levels, while in SiHa cells, inhibition of circ_0001529 expression significantly decreased ERK/MAPK phosphorylation levels (Figure 7B). Subsequently, we added MAPK-specific activator P79350 [16] in si- circ_0001529 group SiHa cells, and Western blot results showed that MAPK and ERK phosphorylation levels were significantly increased (Figure 7C); and cell activity and proliferation rate were significantly enhanced (Figures 7D-7F). Apoptosis was significantly attenuated (Figures 7G-7I); and cell cycle arrest was effectively alleviated (Figure 7J).

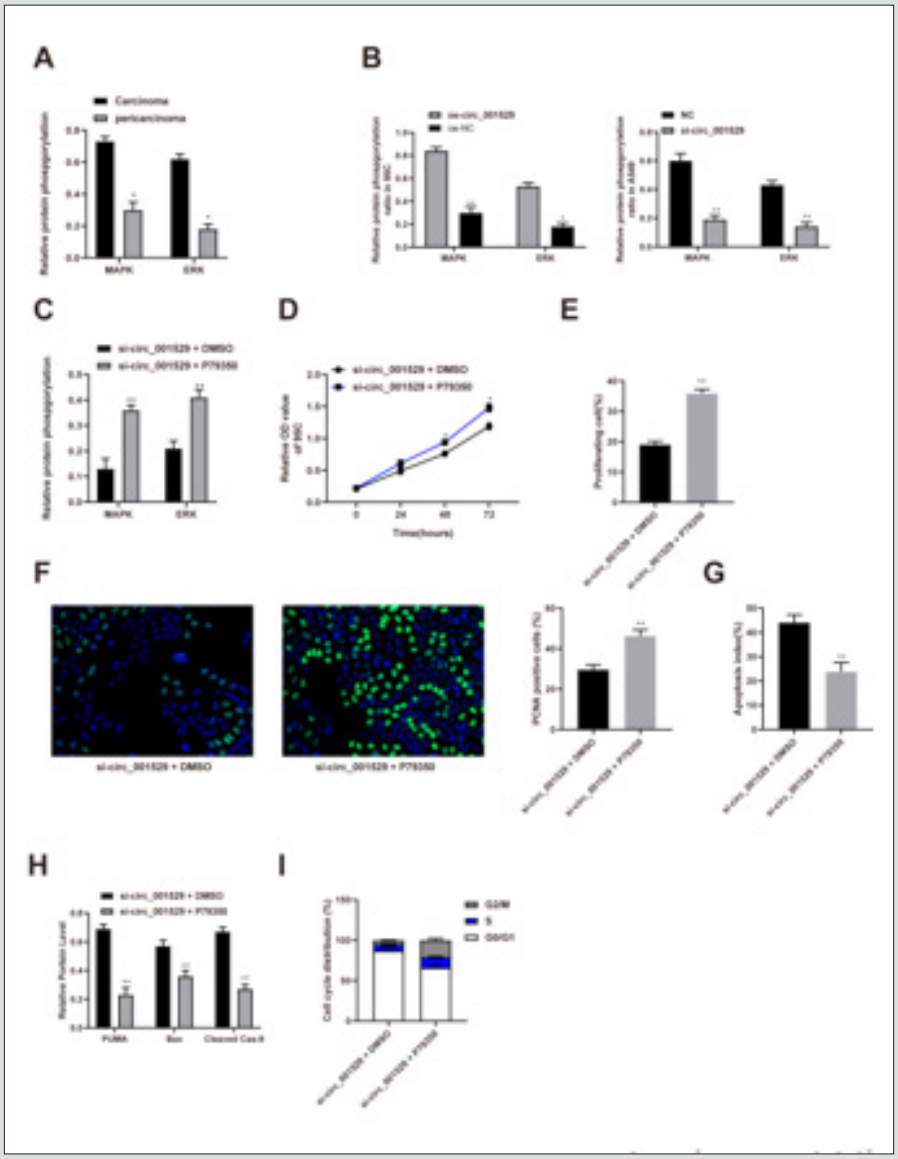


**Figures 7:** CDC25A promotes ovarian carcinogenesis through upregulation of ERK/MAPK signaling pathway. (A) ERK/MAPK signaling pathway expression in cancer and paracancer tissues; (B) ERK/MAPK signaling pathway expression in SKOV3 cells and SiHa cells; (c) ERK/MAPK signaling pathway expression in SiHa cells after addition of MAPK activator P79350; (D) MTT assay for cell activity; (E) Cell proliferation. (F) PCNA immunofluorescence staining; (G) Apoptosis situation; (H) CytC staining; (I) Apoptosis-related protein detection; (J) Cell cycle distribution.

## Discussion

Ovarian cancer (OC) is the deadliest gynecological malignancy, and little is known about its underlying tumorigenesis mechanism [17]. In 2018 alone, over 295,000 women developed OC, of whom over 184,000 died globally [18]. To date, OC is still the lowest survival rate of all gynecological malignancies, because it is usually diagnosed at an advanced stage. This may be due to a lack of effective tumor biomarkers [1]. Among the candidate sponges, we elucidated the association of circ_0001529 with miR-578. In addition, we demonstrated that miR-578 directly targets circ_0001529. Functionally, we established experimental systems to investigate the effects of miR-578 interactions in vitro and in vivo. This study assessed that knockdown of circ_0001529 promotes apoptosis in ovarian cancer cells and provides a new therapeutic target for ovarian cancer. A growing body of evidence suggests that ncRNAs, including miRNAs, lncRNAs, and circRNAs, play an indispensable role in the initiation and progression of OC. [1] Due to the difficulty of delivering ncRNAs, people are striving to explore engineered exosomal miRNA replacement therapy. In other words, exosomes are purified from omental fibroblasts of OC patients, and tumor-inhibiting miRNAs are selected and electroporated into exosomes to inhibit tumor proliferation and invasion.

[1] Studies have shown that circRNA is involved in the occurrence of tumors in many ways, so it can be used as a molecular marker for tumor diagnosis and treatment [19]. Firstly, in this manuscript, the expression of Circ_0001529 in ovarian cancer tissues and cell lines was detected by qRT-PCR and Western blot. Dual luciferase was used to validate the target of Circ_0001529 and silencing and overexpression of Circ_0001529 in cell lines were used to explore its relationship with miR-578. The expression level of ACP5 was examined by qRT-PCR. Taken together, our results suggest that circ-LOPD2 acts as a sponge for miR-378 to promote the proliferation of ovarian cancer cells, which in turn may promote the development of OC. Then, in order to obtain the relationship between Circ_0001529 being highly expressed in ovarian cancer tissues and cells, obtained by online database analysis, the relationship between the expression of Circ_0001529 and the clinical characteristics of ovarian cancer patients was analyzed. Meantime, Circular RNAs (circRNAs) are increasingly recognized as an important regulator of cancer including ovarian cancer (OC), and patients with high expression of Circ_0001529 have a poor prognosis.8 The focus of this work is the influence of circ_0001529 on the development of OC and the molecules involved. Studies have shown that curcumin inhibits the proliferation of ovarian cancer and promotes apoptosis by regulating the circ-PLEKHM3/miR-320a/SMG1 axis. [20] Moreover, circ-LOPD2 acts as a miR-378 sponge to promote the proliferation of ovarian cancer cells, which may in turn promote the development of OC19 and circ_0000554 was overexpressed in ovarian tumor specimens and cells [21]. All of these successful studies play an important role in our Circ_0001529 exploration and impact on OC.

Subsequently, many studies described the cytoplasmic location of circRNAs and the sponge effect of circRNAs on miRNAs, which further led to gene regulation at the post-transcriptional level, thereby promoting the development of cancer [22]. Herein, to further validate the role of Circ_0001529 in ovarian cancer, qRT-PCR was used to detect the mRNA expression level, and in the same way, the experiment could also detect the expression level of Circular RNAs (circRNAs). The results showed that the expression of Circ_0001529 was interfered, indicating that the transfection was successful. the expression level of Circ_0001529 was significantly increased in ovarian cancer tissues, which played a significant role in the metastasis and progression of cancer cells.

Meanwhile, silencing CDC25A can inhibit the proliferation of ovarian cancer cells and promote cell apoptosis. Some experiments have shown that miR-34a-5p regulates the growth, migration and other malignant behaviors of CC [23]. Detection by flow cytometry revealed that overexpression of CDC25A significantly reduced the expression level of apoptosis-related proteins, and overexpression of Circ_0001529 did not lead to cell cycle arrest, indicating that inhibition of CDC25A expression promotes G2/M phase cycle arrest. Trichodermin regulated the expression of Cdc25A and its downstream proteins via c-Myc. Overexpression of c-Myc attenuated trichodermin's anti-ovarian cancer activity [24]. Mechanically, CDC25A hinders the cell cycle progression of MCS cells, enhances its structural integrity, and maintains the up-regulation of E-cadherin in MCS cells. Therefore, the addition of NSC95397, a small molecule inhibitor of CDC25A, makes MCS of ovarian cancer sensitive to chemotherapy drugs. This provides us with a new strategy for the treatment of peritoneal metastasis of ovarian cancer and may help improve the overall health of patients with ovarian cancer [25]. Finally, to further obtain that expression of Circ_0001529 promotes the growth of heterotopic tumors in mice in vivo, the expression levels and phosphorylation levels of ERK/MAPK in cancer and paracancerous tissues were detected by Western Blot, and CDC25A promotes ovarian carcinogenesis through upregulation of the ERK/MAPK signaling pathway. Moreover, these findings were accompanied by decreased protein levels of CDK2, CDC25A, PKA, p-AMPK, and eEF2K, as well as increased protein levels of cyclin A, cleaved caspase-3, caspase-8, and caspase-9.26 In conclusion, our results suggest that ERK/MAPK is significantly overexpressed in most cancers, with synergistic anticancer activity in OC cells. Therefore, the combination of Circ_0001529 and miR-578-targeted therapy may be promising in the future to improve the response of cancer cells.

## Limitation

We still have some limitations, such as small sample size, we did not generalize to all types of ovarian cancer, and this study did not describe follow-up characteristics. We need more large-scale randomized double-blind controlled trials to overcome the methodological and reporting shortcomings. In addition, all studies were not reported blinded. The risk of bias was unclear in most trials. In addition to studying correlations between sample size and Circ_0001529, correlations between miR-578 and CDC25A mRNA, but correlations from univariate and multiple meta-regression analyses were missing. Finally, limited useful methods and tools exist for OC, and for Circ_0001529, which is a circular RNA, is a newly explored research idea for us, which still needs several practice sessions to ensure the most accurate experimental results. Overall, all these limitations may have led to an inadequate assessment of the results.

## Conclusion

Circ_0001529 is highly expressed in ovarian cancer tissues and cells; silencing Circ_0001529 inhibits ovarian cancer cell growth and promotes apoptosis in vitro and in vivo, and vice versa. circ_0001529 can bind to miR-578 target and miR-578 binds to CDC25A mRNA target. Overexpression of Circ_0001529 promotes the expression of CDC25A and promotes the growth and inhibits the apoptosis of ovarian cancer cells. cdc25A can upregulate the ERK/MAPK signaling pathway, thus promoting ovarian carcinogenesis. Silencing Circ_0001529 in ovarian cancer cell disease will undoubtedly provide new diagnostic opportunities and therapeutic targets for drug discovery.

## References


1. Zhang Y, Wei YJ, Zhang YF, Liu HW, Zhang YF (2021) Emerging Functions and Clinical Applications of Exosomal ncRNAs in Ovarian Cancer. Front Oncol 11: 765458.
2. Sastra WIG, Aditya PPK, Gradiyanto OE, Ketut S (2021) Predictive value of preoperative inflammatory markers and serum CA 125 level for surgical outcome in Indonesian women with epithelial ovarian cancer. Cancer Biomark.
3. Zhu Cheng, Zhang Nenghua, Zhong Ailing, Xiao Kangjia, Lu Renquan, Guo Lin (2021) A combined strategy of TK1, HE4 and CA125 shows better diagnostic performance than Risk of Ovarian Malignancy Algorithm (ROMA) in ovarian carcinoma. Clinica Chimica Acta; International Journal of Clinical Chemistry 524(3).
4. Antonio Cascales Campos Pedro, Alida González Gil, Elena Gil Gómez, Rocío González Sánchez, Jerónimo Martínez García (2021) Cytoreductive Surgery with or Without HIPEC After Neoadjuvant Chemotherapy in Ovarian Cancer: A Phase 3 Clinical Trial. Ann Surg Oncol.
5. Wei Wei, Feng Zhanzhan, Liu Zhihao, Li Xinyue, He Hualong (2021) Design, synthesis and biological evaluation of 7-((7H-pyrrolo[2,3-d] pyrimidin-4-yl) oxy)-2,3-dihydro-1H-inden-1-one derivatives as potent FAK inhibitors for the treatment of ovarian cancer. Eur J Med Chem 228: 113978.
6. Huang Weiyi, Chen Lili, Sun Pengming (2021) ERRα expression in ovarian cancer and promotes ovarian cancer cells migration in vitro. Arch Gynecol Obstet.
7. Li B, Zhang L (2021) CircSETDB1 knockdown inhibits the malignant progression of serous ovarian cancer through miR-129-3p-dependent regulation of MAP3K3. J Ovarian Res 14(1): 160.
8. Wang S (2021) RNA-binding protein IGF2BP2 enhances circ_0000745 abundancy and promotes aggressiveness and stemness of ovarian cancer cells via the microRNA-3187-3p/ERBB4/PI3K/AKT axis. J Ovarian Res 14(1): 154.
9. Zada Shah, Lu Huiting, Dai Wenhao, Tang Songsong, Khan Sikandar, et al. (2021) Multiple amplified microRNAs monitoring in living cells based on fluorescence quenching of MoB and hybridization chain reaction. Biosens Bioelectron 197: 113815.
10. Li X, Yang F, Gan C, Yuan R, Xiang Y (2022) Sustainable and cascaded catalytic hairpin assembly for amplified sensing of microRNA biomarkers in living cells. Biosens Bioelectron 197: 113809.
11. Wu A (2020) Upregulated hsa_circ_0005785 Facilitates Cell Growth and Metastasis of Hepatocellular Carcinoma Through the miR-578/APRIL Axis. Front Oncol 10: 1388.
12. Ji Yanlei, Han Zhen, Shao Limei, Zhao Yuehuan (2016) Evaluation of in vivo antitumor effects of low-frequency ultrasound-mediated miRNA-133a microbubble delivery in breast cancer. Cancer Med 5(9): 2534-2543.
13. Huang Chengqun, Liu Wayne, Perry Cynthia N, Yitzhaki Smadar, Lee Youngil, et al. (2010) Autophagy and protein kinase C are required for cardioprotection by sulfaphenazole. Am J Physiol Heart Circ Physiol 298(2): H570-H579.
14. Yoo Jeong Ju, Lee Jeong Hoon, Lee Sang Hwan, Lee Minjong, Lee Dong Hyeon, et al. (2014) Comparison of the effects of transarterial chemoembolization for advanced hepatocellular carcinoma between patients with and without extrahepatic metastases. PLoS One 9(11): e113926.
15. Leng Feng, Saxena Lovely, Hoang Nam, Zhang Chunxiao, Lee Logan, et al. (2018) Proliferating cell nuclear antigen interacts with the CRL4 ubiquitin ligase subunit CDT2 in DNA synthesis-induced degradation of CDT1. J Biol Chem 293(49): 18879-18889.
16. Lv Bochang, Huo Fuquan, Dang Xiaojie, Xu Zhiguo, Chen Tao, et al. (2016) Puerarin Attenuates N-Methyl-D-aspartic Acid-induced Apoptosis and Retinal Ganglion Cell Damage Through the JNK/p38 MAPK Pathway. J Glaucoma 25(9): e792-801.
17. Giudice Elena, Salutari Vanda, Ricci Caterina, Nero Camilla, Carbone Maria Vittoria, et al. (2021) Gut microbiota and its influence on ovarian cancer carcinogenesis, anticancer therapy and surgical treatment: A literature review. Crit Rev Oncol Hematol 168: 103542.
18. Hou C, Jiang ZZ, Pan B, Zhang XC, Liu YQ (2021) A Comparison of Chemotherapy Used with and without Apatinib for Patients with Ovarian Carcinoma Who Progressed after Standard Regimens: A Systematic Review and Meta-Analysis. Evid Based Complement Alternat Med 2021: 2292907.
19. Wei X, Lv H, Yang S, Yang X (2021) CircRNA PLOD2 enhances ovarian cancer propagation by controlling miR-378. Saudi J Biol Sci 28: 6260-6265.
20. Sun S, Fang H (2021) Curcumin inhibits ovarian cancer progression by regulating circ-PLEKHM3/miR-320a/SMG1 axis. J Ovarian Res 14(1): 158.
21. Wang H, Zhang X, Qiao L, Wang H (2021) CircRNA circ_0000554 promotes ovarian cancer invasion and proliferation by regulating miR-567. Environ Sci Pollut Res Int.
22. Huang X, Luo Y, Li X (2021) Circ_0072995 Promotes Ovarian Cancer Progression Through Regulating miR-122-5p/SLC1A5 Axis. Biochem Genet.
23. Jiang T, Cheng H (2021) miR-34a-5p blocks cervical cancer growth and migration by downregulating CDC25A. J BUON 26(5): 1768-1774.
24. Gao Ying, Miles Sarah L, Dasgupta Piyali, Rankin Gary O, Cutler Stephen, et al. (2021) Trichodermin Induces G0/G1 Cell Cycle Arrest by Inhibiting c-Myc in Ovarian Cancer Cells and Tumor Xenograft-Bearing Mice. Int J Mol Sci 22(9).
25. Sun Y (2019) CDC25A Facilitates Chemo-resistance in Ovarian Cancer Multicellular Spheroids by Promoting E-cadherin Expression and Arresting Cell Cycles. J Cancer 10: 2874-2884.
26. Gao M, Deng C, Dang F (2021) Synergistic antitumor effect of resveratrol and sorafenib on hepatocellular carcinoma through PKA/AMPK/eEF2K pathway. Food Nutr Res 65.

**DOI:** 10.32474/IGWHC.2022.05.000206